

Statistical mechanics of the inverse Ising problem and the optimal objective function

Johannes Berg*

Institute for Theoretical Physics, University of Cologne, Zùlpicher StraÙe 77, 50937 Cologne, Germany

The inverse Ising problem seeks to reconstruct the parameters of an Ising Hamiltonian on the basis of spin configurations sampled from the Boltzmann measure. Recently, strategies to solve the inverse Ising problem based on convex optimisation have proven to be very successful. These approaches maximize particular objective functions with respect to the model parameters. Examples are the pseudolikelihood method and interaction screening. In this paper, we establish a link between approaches to the inverse Ising problem based on convex optimisation and the statistical physics of disordered systems. We characterize the performance of an arbitrary objective function and calculate the objective function which optimally reconstructs the model parameters. We evaluate the optimal objective function within a replica-symmetric ansatz and compare the results of the optimal objective function with other reconstruction methods. Apart from giving a theoretical underpinning to solving the inverse Ising problem by convex optimisation, the optimal method outperforms state-of-the-art methods, in some regimes by a significant margin.

PACS numbers: 02.30.Zz, 02.50.Tt, 89.75.-k 75.50.Lk

The advent of large-scale data across different scientific disciplines, especially biology, has inspired many applications of the inverse Ising problem. Over the last decade, the inverse Ising problem has been used to analyze neural firing patterns [1], to determine the three-dimensional structure of proteins [2], to infer biological fitness landscapes [3, 4], and to analyze financial data [5]. This versatility is not surprising: the inverse Ising problem arises naturally when one wants to learn the interactions between discrete variables describing an equilibrium system.

Conceptually, the inference of parameters of an Ising model from data is a simple matter: Consider an Ising model with N binary spin variables, $s_i = \pm 1, i = 1, \dots, N$. Pairwise interactions between the spins lead to the well-known Ising Hamiltonian

$$\mathcal{H} = - \sum_{i < j} \frac{J_{ij}^*}{\sqrt{N}} s_i s_j, \quad (1)$$

where $\frac{J_{ij}^*}{\sqrt{N}}$ quantifies the coupling strength between a pair of spins, which we seek to infer. We have inserted a constant $1/\sqrt{N}$ for later convenience, magnetic fields can also be added without difficulty. M spin configurations (samples) $\mathbf{s}^1, \dots, \mathbf{s}^M$ are drawn independently from the Boltzmann distribution

$$P_B(\mathbf{s}|\mathbf{J}^*) = \frac{1}{Z^*(\mathbf{J}^*)} \exp \left\{ \sum_{i < j} \frac{J_{ij}^*}{\sqrt{N}} s_i s_j \right\}, \quad (2)$$

and the task is to find the couplings which produce these spin configurations. This can be done by maximizing the so-called log-likelihood

$$\sum_{\mu=1}^M \ln P_B(\mathbf{s}^\mu|\mathbf{J}) = \sum_{i < j} \frac{J_{ij}}{\sqrt{N}} \sum_{\mu=1}^M s_i^\mu s_j^\mu - M \ln Z^*(\mathbf{J}), \quad (3)$$

with respect to the couplings, which yields the maximum-likelihood estimate of the couplings. Alternatively, Bayes theorem specifies a probability distribution over the reconstructed couplings

$$P(\mathbf{J}|\mathbf{s}^1, \dots, \mathbf{s}^M) = \frac{\prod_{\mu=1}^M P_B(\mathbf{s}^\mu|\mathbf{J}) P(\mathbf{J})}{P(\mathbf{s}^1, \dots, \mathbf{s}^M)} \quad (4)$$

called the posterior probability. One can reconstruct the couplings by maximizing this posterior probability with respect to the couplings, or by computing their expected value under the posterior. In the limit of a large number of samples $M/N \rightarrow \infty$, maximizing the Bayesian posterior (4) yields the same couplings as maximizing the log-likelihood (3).

In practice, however, the computation of either the likelihood or the Bayesian posterior is a hard task: the Boltzmann distribution (2) contains the partition function, whose computations requires a number of steps which scales exponentially with the system size. A large number of approaches to likelihood maximisation have been made using the tools of statistical physics, including Monte Carlo methods for small systems [6], the mean field approximation [7], a small-correlation expansion [8], and others. However, one of the most successful methods to solve the inverse Ising problem sidesteps the computation of the the likelihood altogether. It originates from statistics and is called pseudolikelihood [9–11]. Pseudolikelihood reconstruction proceeds by maximizing

$$\begin{aligned} \sum_{\mu} s_i^\mu \sum_{j \neq i} \frac{J_{ij}}{\sqrt{N}} s_j^\mu - \ln \left(2 \cosh \left(\sum_j \frac{J_{ij}}{\sqrt{N}} s_j^\mu \right) \right) \\ = \sum_{\mu} k_i^\mu - \ln(2 \cosh k_i^\mu) = \sum_{\mu} \rho(k_i^\mu) \end{aligned} \quad (5)$$

with respect to the couplings, or rather, with respect to a particular row $J_{i\bullet}$ of the matrix of couplings. In (5),

we have introduced a shorthand describing spins coupled their effective local field $k_i^\mu \equiv s_i^\mu \sum_{j \neq i} \frac{J_{ij}}{\sqrt{N}} s_j^\mu$, as well as the pseudolikelihood objective function $\rho(k) = k - \ln(2 \cosh k)$. This method can be interpreted as using a paramagnetic model to describe the statistics of one particular spin s_i in an effective local field, which depends on the couplings between spins. Pseudolikelihood reconstruction has a number of attractive features: the couplings can be determined row-by-row using a convex optimisation algorithm, and the reconstruction becomes exact in the limit $M/N \rightarrow \infty$, even at low temperatures where many other methods fail [11].

Recently, a different function has been proposed as an objective function, $\rho(k) = e^{-k}$:

$$\sum_{\mu} e^{-s_i^\mu \sum_j \frac{J_{ij}}{\sqrt{N}} s_j^\mu} = \sum_{\mu} e^{-k_i^\mu} \quad (6)$$

is to be minimized over the row $J_{i\bullet}$ of the matrix of couplings [12]. This reconstruction method, termed interaction screening, outperforms pseudolikelihood when the underlying coupling matrix is sparse, and comes close to saturating bounds on reconstruction set by information theory [13].

Both pseudolikelihood and interaction screening are heuristics, so one can ask if there is an objective function $\rho_{\text{opt}}(k)$, which reconstructs the parameters of the Ising model optimally, that is, minimizes the difference between the reconstructed and underlying couplings over all functions $\rho(k)$ that one might use. In this paper, we build a statistical mechanics of the inverse Ising problem based on the family of objective functions $\rho(k)$. This theory tells us how well a certain objective function reconstructs the underlying couplings. It can also be used to derive the objective function which performs best. The theory applies to typical realisations of the underlying couplings, which in the thermodynamic limit $N \rightarrow \infty$ are realised in nearly all instances of the couplings drawn from a particular distribution. For simplicity, we restrict ourselves to coupling matrices whose entries are drawn independently from a Gaussian distribution.

We start by considering an arbitrary (convex) objective function $\rho(k)$. For the first row of the coupling matrix $\mathbf{J}_1 = \{J_{1j}\}$ (and equivalently for all other rows) we obtain the minimum of the objective function

$$\begin{aligned} \min_{\{J_{1j}\}} & \left[\sum_{\mu=1}^M \rho\left(\frac{s_1^\mu}{\sqrt{N}} \sum_{j \neq i} J_{1j} s_j^\mu\right) \right] \\ &= - \lim_{\beta \rightarrow \infty} \partial_\beta \ln \int d\mathbf{J}_1 e^{-\beta \sum_{\mu=1}^M \rho(k_1^\mu)} \\ &= - \lim_{\beta \rightarrow \infty} \partial_\beta \ln Z(\mathbf{s}^1, \mathbf{s}^2, \dots, \mathbf{s}^M), \end{aligned} \quad (7)$$

where we have defined a partition function $Z(\mathbf{s}^1, \dots, \mathbf{s}^M) = \int d\mathbf{J}_1 e^{-\beta \sum_{\mu=1}^M \rho(k_1^\mu)}$ for the inverse problem. In this partition function, the exponential

function plays the role of a Boltzmann weight, from which the limit $\beta \rightarrow \infty$ selects the ground state thus minimizing $\sum_{\mu=1}^M \rho(k_1^\mu)$. The M spins samples $\mathbf{s}^1, \dots, \mathbf{s}^M$ are taken independently from the Boltzmann distribution (2). They remain fixed while the minimum over \mathbf{J}_1 is sought and can be considered as quenched disorder. Conversely, the entries of the reconstructed matrix of couplings act as phase space variables and are integrated out while spin samples remain constant. The logarithm of the partition function averaged over the disorder, the so-called quenched average, is

$$\begin{aligned} \langle \ln Z(\mathbf{s}^1, \dots, \mathbf{s}^M) \rangle &= \prod_{i < j} \int \frac{dJ_{ij}^*}{\sqrt{2\pi q^*}} \exp \left\{ -\frac{1}{2q^*} \sum_{i < j} J_{ij}^{*2} \right\} \\ &\quad \prod_{\mu} \left(\frac{1}{Z^*(\mathbf{J}^*)} \sum_{\mathbf{s}^\mu} \right) \exp \left\{ \sum_{i < j, \mu} \frac{J_{ij}^*}{\sqrt{N}} s_i^\mu s_j^\mu \right\} \\ &\quad \ln \left(\int d\mathbf{J}_1 \exp \left\{ -\beta \sum_{\mu} \rho\left(\frac{s_1^\mu}{\sqrt{N}} \sum_{j \neq i} J_{1j} s_j^\mu\right) \right\} \right), \end{aligned} \quad (8)$$

where the double pointed brackets indicate the average both over the underlying couplings and samples. q^* is the variance of the underlying couplings. We use the replica-trick in two different places of the calculation: to represent the logarithm of the partition function $Z(\mathbf{s}^1, \dots, \mathbf{s}^M)$ and to compute one over the partition function $Z^*(\mathbf{J}^*)$ in the Boltzmann measure. Details can be found in the appendix. Under a replica-symmetric ansatz we take the low-temperature limit $\beta \rightarrow \infty$ and the thermodynamic limit $N \rightarrow \infty$ and find the free energy

$$\begin{aligned} -f &= \lim_{\beta \rightarrow \infty} \frac{1}{\beta} \langle \ln Z(\mathbf{s}^1, \dots, \mathbf{s}^M) \rangle \\ &= \text{extr}_{q, v, R} \left[\frac{q - R^2/q^*}{2v} - \alpha \int Dt \mathcal{M}_v[\rho](R + \sqrt{q}t) \right], \end{aligned} \quad (9)$$

with $Dt = \frac{dt}{\sqrt{2\pi}} e^{-t^2/2}$ and $\alpha = M/N$. The free energy is evaluated by extremizing over the order-parameters q , R and v .

$$\mathcal{M}_v[\rho](x) = \min_k \left[\frac{(k - x)^2}{2v} + \rho(k) \right] \quad (10)$$

defines the so-called Moreau envelope of $\rho(k)$, which plays an important role in convex optimisation and nonlinear analysis [14]. The minimum over k in (10) seeks to minimize $\rho(k)$ while at the same time staying close to x , with the relative weight of these two objectives being controlled by v . The Moreau envelope also appears in the context of optimal linear regression [15–17], where it emerges in a statistical mechanics analysis as well [18].

The order parameters q and R appearing in the free energy (9) describe the statistics of the reconstructed cou-

plings. At the extremum (9), the order parameter

$$R = \frac{1}{N} \sum_j \langle\langle J_{1j} J_{1j}^* \rangle\rangle \quad (11)$$

describes the overlap between the reconstructed couplings and the underlying couplings. Similarly, the order parameter

$$q = \frac{1}{N} \sum_j \langle\langle J_{1j} J_{1j} \rangle\rangle \quad (12)$$

gives the overlap between a row vector of reconstructed couplings and itself. These order parameters turn out to be self-averaging in the thermodynamic limit: although $\frac{1}{N} \sum_j J_{1j} J_{1j}$ fluctuates between different realisations of the couplings \mathbf{J}^* and the samples, these fluctuations vanish with increasing system size, so for (nearly) all realisations of the disorder we have $\frac{1}{N} \sum_j J_{1j} J_{1j} = \frac{1}{N} \sum_j \langle\langle J_{1j} J_{1j} \rangle\rangle$, and similarly for the overlap R .

The distribution of the reconstructed couplings can also be calculated from the partition function (8), see appendix. Collecting all spin pairs where the underlying coupling takes on a particular value J^* , the corresponding reconstructed couplings turn out to follow a Gaussian distribution with mean $\frac{RJ^*}{q^*}$ and a variance $q - R^2/q^*$. For the reconstruction to have no bias, the overlap R thus needs to equal the variance of the underlying couplings q^* .

The two order parameters R and q also specify the reconstruction error. We look at the relative mean-square error

$$\epsilon = \frac{\sum_i (J_{1i} - J_{1i}^*)^2}{\sqrt{(\sum_i J_{1i}^2)(\sum_i J_{1i}^{*2})}} = \frac{q - 2R + q^*}{\sqrt{qq^*}}. \quad (13)$$

and seek the particular objective function $\rho_{\text{opt}}(k)$, which minimizes this error. Using the calculus of variations applied to the free energy (9), we find

$$\rho_{\text{opt}}(k) = k^2 - 2\delta k, \quad (14)$$

a square function with a non-trivial offset, whose value is $\delta = (1 + q^*) \sqrt{\frac{q^*(\alpha-1)}{\alpha q^* + 1}}$, see appendix for details. Error measures different from (13) which also depend on the order parameters R and q yield the same quadratic form of the optimal objective function, but have different values of δ . Finding the optimal objective function requires the variance q^* of the unknown couplings. q^* and hence the offset can be determined as follows: For the objective function (14), the free energy (9) can be calculated easily, giving the overlap parameters

$$R = \frac{q^* \delta}{1 + q^*} \quad (15)$$

$$q = \frac{(\alpha q^* + 1) \delta^2}{(1 + q^*)^2 (\alpha - 1)}. \quad (16)$$

The overlap $q = \frac{1}{N} \sum_j J_{1j}^2$ of reconstructed couplings can be calculated easily without knowing the underlying couplings. q^* and thus the optimal value of the offset δ can thus be determined from a simple linear fit of q against δ^2 . In Figure 1, we treat the offset δ as a free parameter and show the reconstruction error (13) as well as the overlaps R and q for different values of δ and compare them to numerical simulations.

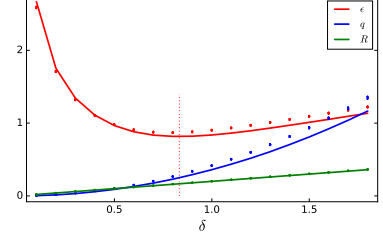


FIG. 1. **Reconstruction with the optimal objective function** (14). The overlaps R and q given by (15) and (16) and the reconstruction error ϵ defined by (13) are plotted against the offset δ in green, blue, and red, respectively (bottom to top). The numerical results were obtained by reconstructing a single system of $N = 100$ spins: The underlying couplings J_{ij}^* were drawn independently from a Gaussian with mean zero and variance $q^* = 0.25$. Next, $M = 500$ samples ($\alpha = M/N = 5$) were generated by independent Monte-Carlo runs with a breaking-in time of 100 Monte-Carlos sweeps each to ensure equilibrium had been reached. To reconstruct the couplings, the optimal objective function (14) was minimized over separate rows of the coupling matrix using the `NLOpt` package in Julia using Newton's method `LD_TNEWTON`. The overlap parameters R and q and the reconstruction error ϵ were computed row-by-row. We plot averages over rows with the standard error as error bars (smaller than the symbol size). The vertical line indicates the value of $\delta = (1 + q^*) \sqrt{\frac{q^*(\alpha-1)}{\alpha q^* + 1}}$ which minimizes the reconstruction error.

Figure 2 compares reconstructed and underlying couplings for different methods; the optimal objective function (14), pseudolikelihood (5), and mean-field reconstruction [7], showing that the optimal objective function (14) outperforms both of these methods. Figure 3 compares the reconstruction error (13) for these three methods, as well as interaction screening (6), at different values of $\alpha = M/N$. The optimal objective function performs best, with a particularly wide margin at low values of α . The reconstruction error increases for all four methods as α decreases, most rapidly for pseudolikelihood, interaction screening, and mean-field reconstruction. For mean-field reconstruction, the rapid increase of the reconstruction error with decreasing α is connected to the matrix of two-point spin correlations becoming singular at $\alpha = 1$. For mean-field reconstruction, but also for the reconstruction based on pseudolikelihood and interaction screening, we find that the self-overlap parameter q diverges as α approaches one from above [19]. For pseudolikelihood and interaction screening, this divergence can

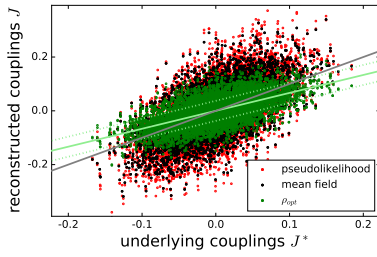


FIG. 2. Reconstructed couplings versus underlying couplings. The elements J of the reconstructed coupling matrix are plotted against the corresponding underlying couplings J^* . Parameters and numerical procedures are the same as in Fig. 1. Perfect reconstruction $J = J^*$ is indicated by the grey line along the diagonal. The results from the optimal objective function (14) are shown in green, the reconstruction using pseudolikelihood (5) in red. Black dots show the results of mean-field reconstruction $\mathbf{J} = -\chi^{-1}$, where χ is the matrix of connected two-point correlations [7]. The light green lines show the statistics of the reconstructed couplings calculated analytically; the solid line $J = \frac{R J^*}{q^*}$ gives the mean reconstructed couplings, the dotted lines are one standard deviation above and below that mean.

in principle be avoided by adding a regularizing term $\frac{\gamma}{2} \sum_j J_{1j}^2$ to the objective function. However, then the value of the regularisation parameter γ must be determined. This can be done in the same way the value of the offset δ was determined; by re-calculating the overlap parameters q and R with the regularizing term included in the objective function, matching the dependence of q on γ with numerical results to determine q^* , and then solving $q(\gamma) = q^*$ for the regularisation parameter.

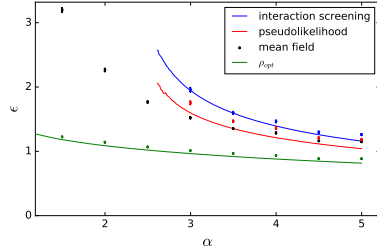


FIG. 3. The reconstruction error ϵ at different numbers of samples. We plot the reconstruction error (13) against the number of samples per spin $\alpha = M/N$. The results from the optimal objective function (14) are shown in green, pseudolikelihood (5) in red, and interaction screening (6) in blue (bottom to top). The corresponding lines give the analytical results based on the free energy (9). Black dots indicate the results of mean-field reconstruction. Parameters and procedures are as in Figure 1, except the optimisation is performed with the algorithm LD_MMA, which turns out to be more stable.

A number of open issues remain, an important one being the validity of the replica-symmetric ansatz used to calculate the free energy (9). At high values of q^* (strong couplings), and also at low values of α , we expect

replica symmetry to be broken, which would lead to an optimal objective function different from (14). Similarly, we expect the small-coupling resummation used to derive the free energy to fail below the spin-glas transition at $q^* = 1$. Another point is the extension of our approach to sparse coupling matrices, which will likely also lead to an optimal objective function different from (14), possibly one close or even identical to interaction screening (6), which performs very well in the regime of sparse couplings matrices [12].

Acknowledgments: Many thanks to Guy Bunin, David Gross, and Chau Nguyen for discussions.

* berg@thp.uni-koeln.de

- [1] E. Schneidman, M. J. Berry, R. Segev, and W. Bialek, *Nature* **440**, 1007 (2006).
- [2] M. Weigt, R. A. White, H. Szuromant, J. A. Hoch, and T. Hwa, *Proc. Natl. Acad. Sci. USA* **106**, 67 (2009).
- [3] T. Mora, A. M. Walczak, W. Bialek, and C. G. Callan, *Proc. Natl. Acad. Sci. USA* **107**, 5405 (2010).
- [4] K. Shekhar, C. F. Ruberman, A. L. Ferguson, J. P. Barton, M. Kardar, and A. K. Chakraborty, *Phys. Rev. E* **88**, 062705 (2013).
- [5] T. Bury, *Physica A: Statistical Mechanics and its Applications* **392**, 1375 (2013).
- [6] T. Broderick, M. Dudik, G. Tkacik, R. E. Schapire, and W. Bialek, *arXiv preprint arXiv:0712.2437* (2007).
- [7] H. J. Kappen and F. Rodríguez, *Advances in Neural Information Processing Systems*, 280 (1998).
- [8] V. Sessak and R. Monasson, *J. Phys. A: Math. Theor.* **42**, 055001 (2009).
- [9] J. Besag, *J. R. Stat. Soc. B* **36**, 192 (1974).
- [10] P. Ravikumar, M. J. Wainwright, and J. D. Lafferty, *Ann. Stat.* **38**, 1287 (2010).
- [11] E. Aurell and M. Ekeberg, *Phys. Rev. Lett.* **108**, 090201 (2012).
- [12] M. Vuffray, S. Misra, A. Y. Lokhov, and M. Chertkov, *arXiv preprint arXiv:1605.07252* (2016).
- [13] N. P. Santhanam and M. J. Wainwright, *IEEE Transactions on Information Theory* **58**, 4117 (2012).
- [14] N. Parikh and S. Boyd, *Found. Trends Optim.* **1**, 127 (2014).
- [15] N. El Karoui, D. Bean, P. J. Bickel, C. Lim, and B. Yu, *Proceedings of the National Academy of Sciences* **110**, 14557 (2013).
- [16] D. Bean, P. J. Bickel, N. El Karoui, and B. Yu, *Proceedings of the National Academy of Sciences* **110**, 14563 (2013).
- [17] D. Donoho and A. Montanari, *Probability Theory and Related Fields*, 1 (2013).
- [18] M. Advani and S. Ganguli, *Phys. Rev. X* **6**, 031034 (2016).
- [19] For α below three, the convex optimisation fails for pseudolikelihood and interaction screening and also the numerical extremization of the free energy (9) fails.
- [20] T. L. Watkin, A. Rau, and M. Biehl, *Reviews of Modern Physics* **65**, 499 (1993).
- [21] A. Engel and C. Van den Broeck, *Statistical mechanics of learning* (Cambridge University Press, 2001).

APPENDIX

1. Computing the partition function

To average $\ln Z(\mathbf{s}^1, \mathbf{s}^2, \dots, \mathbf{s}^M)$ in (8) over the disorder, we use the replica trick in two separate instances. First, to represent the logarithm of the partition function in (7), we use $\ln Z = \lim_{n \rightarrow 0} \partial_n Z^n$. The inverse of the partition function in Boltzmann distribution (2) is represented with a second set of replicas based on

$$\frac{\sum_{\mathbf{s}} e^{-\beta \mathcal{H}(\mathbf{s})} f(\mathbf{s})}{\sum_{\mathbf{s}} e^{-\beta \mathcal{H}(\mathbf{s})}} = \lim_{m \rightarrow 0} \prod_{\alpha=1}^m \left(\sum_{\mathbf{s}^\alpha} e^{-\beta \sum_{\alpha} \mathcal{H}(\mathbf{s}^\alpha)} f(\mathbf{s}^1) \right). \quad (17)$$

Taking the underlying couplings J_{ij}^* to be taken independently from a Gaussian distribution with zero mean and variance q^* the average of $Z^n(\mathbf{s}^1, \dots, \mathbf{s}^M)$ is

$$\begin{aligned} \langle\langle Z^n(\mathbf{s}^1, \dots, \mathbf{s}^M) \rangle\rangle &= \prod_{i < j} \int \frac{dJ_{ij}^*}{\sqrt{2\pi q^*}} \exp \left\{ -\frac{1}{2q^*} \sum_{i < j} J_{ij}^{*2} \right\} \\ &\prod_{\mu, \alpha} \left(\frac{1}{2^N} \sum_{\mathbf{s}^{\mu\alpha}} \right) \exp \left\{ \sum_{i < j, \mu, \alpha} \frac{J_{ij}^*}{\sqrt{N}} s_i^{\mu\alpha} s_j^{\mu\alpha} \right\} \\ &\prod_a \left(\int d\mathbf{J}^a \right) \prod_{\mu, a} \left(\int \frac{dk^{\mu a} d\hat{k}^{\mu a}}{2\pi} \right) \exp \left\{ -i \sum_{\mu a} k^{\mu a} \hat{k}^{\mu a} \right\} \\ &\exp \left\{ \frac{i}{\sqrt{N}} \sum_{\mu a} \hat{k}^{\mu a} \sum_{j \neq 1} J_j^a s_j^{\mu 1} - \beta \sum_{\mu a} \rho(k^{\mu a}) \right\}, \end{aligned} \quad (18)$$

where the replica indices a and α run from 1 to n and 1 to m respectively, and the limits $m \rightarrow 0$ and $n \rightarrow 0$ will be taken at the end of the calculation. The vector \mathbf{J} with elements $J_j = J_{1j}$ is the first row of the matrix of inferred couplings. We have used a set of delta-functions to define the argument of the objective function, $k^\mu = s_1^\mu \sum_{j \neq i} J_j s_j^\mu$. Partition functions of this form have been investigated extensively in the context of statistical learning [20, 21]. The key difference here is that the samples $\mathbf{s}^1, \dots, \mathbf{s}^M$ are not generated from some ‘teacher perceptron’, but are taken from the Boltzmann distribution (2).

The partition function (18) can be evaluated by standard techniques, except for the first step, the sum over the samples $s_i^{\mu\alpha}$. Picking out the terms involving the samples, the average factorizes over the sample index μ (which we drop for convenience) leaving

$$\prod_{\alpha} \left(\frac{1}{2^N} \sum_{\mathbf{s}^\alpha} \right) \exp \left\{ \sum_{i < j, \alpha} \frac{J_{ij}^*}{\sqrt{N}} s_i^\alpha s_j^\alpha + \frac{i}{\sqrt{N}} \sum_a \hat{k}^a \sum_j J_j^a s_j^1 \right\}. \quad (19)$$

The contribution from $\alpha = 1$ is

$$\frac{1}{2^N} \sum_{\mathbf{s}^1} \exp \left\{ \frac{1}{\sqrt{N}} \sum_{i < j} s_i^1 (J_{ij}^* + i \sum_a \hat{k}^a J_j^a \delta_{i1}) s_j^1 \right\} = \prod_i \left(\frac{1}{2} \sum_{s_i^1} \right) \exp^{\frac{1}{\sqrt{N}} \sum_{i < j} s_i^1 G_{ij} s_j^1}, \quad (20)$$

where we have introduced the shorthand $G_{ij} = J_{ij}^* + i \sum_a \hat{k}^a J_j^a \delta_{i1}$. Expanding the exponent in a Taylor series (small couplings, *i.e.*, small q^*) gives

$$\prod_i \left(\frac{1}{2} \sum_{s_i^1} \right) \left[1 + \frac{1}{\sqrt{N}} \sum_{i < j} s_i G_{ij} s_j + \frac{1}{2!} \left(\frac{1}{\sqrt{N}} \right)^2 \sum_{i < j} s_i G_{ij} s_j \sum_{k < l} s_k G_{kl} s_l + \dots \right]. \quad (21)$$

The first-order term in this expansion sums to zero, to yield a non-zero result would require $i = j$, which does not appear in the sum. For the second order expression, terms with $i = k, j = l$ sum to $\frac{1}{2!} \sum_{i < j} G_{ij}^2$, other terms either sum to zero or are smaller by a factor of $N^{-1/2}$. For higher-order terms, the dominant contributions come from terms

where spin pairs are contracted in the same manner as in the second-order term. The dominant $(2n)$ -th order term is $\frac{1}{(2n)!N^n}[(2n-1)(2n-3)\dots 3 \times 1] \sum_{i<j} G_{ij}^{2n} = \frac{1}{n!2^n N^n} \sum_{i<j} G_{ij}^{2n}$, resumming the series gives

$$\prod_i^N \left(\frac{1}{2} \sum_{s_i^1} \right) \exp \frac{1}{\sqrt{N}} \sum_{i<j} s_i^1 G_{ij} s_j^1 = \exp \left\{ \frac{1}{2N} \sum_{i<j} G_{ij}^2 \right\}. \quad (22)$$

Expanding the shorthand in this result we have

$$\frac{1}{2N} \sum_{i,j} G_{ij}^2 = \frac{1}{2N} \sum_{i<j} J_{ij}^{*2} + \frac{i}{N} \sum_a \hat{k}^a \sum_j J_{1j}^* J_j^a - \frac{1}{2N} \sum_{a,b} \hat{k}^a \hat{k}^b \sum_j J_j^a J_j^b \quad (23)$$

An analogous calculation can be made for the terms with $\alpha > 1$ which gives

$$\prod_{i=1, \alpha=2}^{N,m} \left(\frac{1}{N} \sum_{s_i^\alpha} \right) \exp \frac{1}{\sqrt{N}} \sum_{i<j, \alpha=2} s_i^\alpha J_{ij}^* s_j^\alpha = \exp \left\{ \frac{m-1}{2N} \sum_{i<j} J_{ij}^{*2} \right\}. \quad (24)$$

In the limit $m \rightarrow 0$ this term cancels with the first term of (23). Note that the first term in (23) scales differently with N from the remaining terms. In order to probe this result numerically at finite N , we compute the averages on the left hand sides (22) and (24) for a single matrix numerically and compare the logarithm of their product (so the first term in (23) cancels with (24)) with the analytical result $+\frac{i}{N} \hat{k} \sum_j J_{1j}^* J_j - \frac{1}{2N} \hat{k}^2 \sum_j J_j J_j$. For $N = 20$, figure 4 compares the numerical average over 2^N samples with the analytical result.

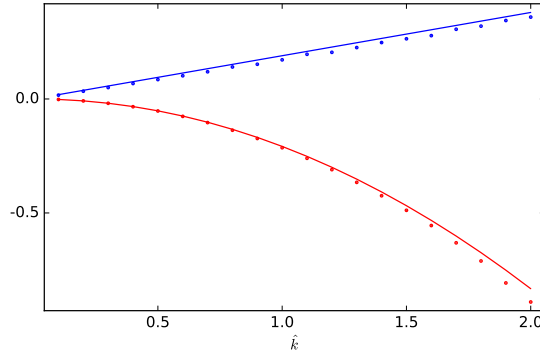


FIG. 4. **The average over samples.** We compare the logarithm of the right and left hand side of the product of equations (22) and (24) as a function of the parameter \hat{k} for $n = 1$ and $m = 0$. J_{ij}^* with $i < j$ are i.i.d. Gaussian entries of zero mean and variance $q^* = 0.25$ and $J_j = J_{1j}^* + x_j$, where the x_j are also i.i.d. Gaussian random variables of zero mean and variance q^* . J_1 is set to zero as it corresponds to a self-interaction. The numerical averages on the left hand sides are indicated by points, the analytical results on the right hand sides are described by lines. As the product of (22) and (24) is complex, real parts are shown in red (bottom), imaginary parts in blue (top).

The remaining terms in (23) can be simplified by introducing the order parameters $q_{ab} = \frac{1}{N} \sum_i J_i^a J_i^b$ and $R^a = \frac{1}{N} \sum_i J_i^a J_{ij}$ via integrals over delta-functions. Thus we obtain in the limit $m \rightarrow 0$

$$\begin{aligned} \langle\langle Z^n(\mathbf{s}^1, \dots, \mathbf{s}^M) \rangle\rangle &= \prod_{i<j} \int \frac{dJ_{ij}^*}{\sqrt{2\pi q^*}} \exp \left\{ -\frac{1}{2q^*} \sum_{i<j} J_{ij}^{*2} \right\} \\ &\prod_{a \leq b} \int \frac{dq_{ab} d\hat{q}_{ab}}{2\pi/N} \prod_a \int \frac{dR_a d\hat{R}_a}{2\pi/N} \exp \{ -iN \sum_{a \leq b} q_{ab} \hat{q}_{ab} - i \sum_a R_a \hat{R}_a \} \\ &\prod_a \int d\mathbf{J}^a \exp \{ +i \sum_{a \leq b} \hat{q}_{ab} \sum_i J_i^a J_i^b + i \sum_a \hat{R}_a \sum_i J_i^a J_{1i}^* \} \\ &\prod_a \int \frac{dk^{\mu a} d\hat{k}^{\mu a}}{2\pi} \exp \{ -i \sum_{\mu a} k^{\mu a} \hat{k}^{\mu a} + i \sum_{\mu a} \hat{k}^{\mu a} R^a - \frac{1}{2} \sum_{a,b,\mu} \hat{k}^{\mu a} \hat{k}^{\mu b} q_{ab} - \beta \sum_{a,\mu} \rho(k^{\mu a}) \} \end{aligned} \quad (25)$$

where the δ -functions themselves were represented by integrals over the so-called conjugate order parameters \hat{q}_{ab} and \hat{R}^a . In the next step, we exploit that the integrals over couplings factorize over $i = 1, \dots, N$ and those over variables $k^{\mu a}$ and $\hat{k}^{\mu a}$ factorize over $\mu = 1, \dots, M = \alpha N$, giving

$$\langle\langle Z^n(\mathbf{s}^1, \dots, \mathbf{s}^M) \rangle\rangle = \prod_{a \leq b} \int \frac{dq_{ab} d\hat{q}_{ab}}{2\pi/N} \prod_a \int \frac{dR_a d\hat{R}_a}{2\pi/N} \exp\{-iN \sum_{a \leq b} q_{ab} \hat{q}_{ab} - iN \sum_a R_a \hat{R}_a + Ng_S(\{\hat{q}_{ab}, \hat{R}^a\}) + \alpha N g_E(\{q_{ab}, R^a\})\}$$

with

$$e^{g_S(\{\hat{q}_{ab}, \hat{R}^a\})} = \int D_{q^*} J^* \prod_a \int dJ^a \exp\{i \sum_{a \leq b} \hat{q}_{ab} J^a J^b + i \sum_a \hat{R}^a J^a J^*\} \quad (26)$$

$$e^{g_E(\{q_{ab}, R^a\})} = \prod_a \int \frac{dk^a d\hat{k}^a}{2\pi} \exp\{-i \sum_a k^a \hat{k}^a + i \sum_a \hat{k}^a R^a - \frac{1}{2} \sum_{a,b} \hat{k}^a \hat{k}^b q_{ab} - \beta \sum_a \rho(k^a)\} \quad (27)$$

where $D_q x = \frac{dx}{\sqrt{2\pi q}} e^{-x^2/(2q)}$ denotes a Gaussian measure with mean zero and variance q . At this point we take a replica symmetric ansatz defined by

$$\begin{aligned} q_{aa} &= q_1 & i\hat{q}_{aa} &= -\frac{1}{2}\hat{q}_1 & \forall a \\ q_{ab} &= q_0 & i\hat{q}_{ab} &= \hat{q}_0 & \forall a < b \\ R_a &= R & i\hat{R}_a &= \hat{R} & \forall a \end{aligned} \quad (28)$$

which allows the evaluation of (26) and the taking of the limit $n \rightarrow 0$ yielding

$$\begin{aligned} -\beta f &\equiv \frac{1}{N} \langle\langle \ln Z(\mathbf{s}^1, \dots, \mathbf{s}^M) \rangle\rangle = \frac{1}{N} \lim_{n \rightarrow 0} \partial_n \langle\langle Z^n(\mathbf{s}^1, \dots, \mathbf{s}^M) \rangle\rangle = \text{extr}_{q_1, \hat{q}_1, q_0, \hat{q}_0, R, \hat{R}} \left[\frac{1}{2} q_1 \hat{q}_1 + \frac{1}{2} q_0 \hat{q}_0 - R \hat{R} \right. \\ &\quad \left. + \frac{1}{2} \ln(2\pi) - \frac{1}{2} \ln(\hat{q}_1 + \hat{q}_0) + \frac{1}{2} \frac{\hat{q}_0 + q^* \hat{R}^2}{\hat{q}_1 + \hat{q}_0} + \alpha \int Dt \ln \left[\int \frac{dk}{\sqrt{2\pi(q_1 - q_0)}} \exp\left\{-\frac{(k - R - \sqrt{q_0}t)^2}{2(q_1 - q_0)} - \beta \rho(k)\right\} \right] \right]. \end{aligned} \quad (29)$$

The extremum over the conjugate order parameters $\hat{q}_1, \hat{q}_0, \hat{R}$ can be evaluated easily yielding

$$\hat{q}_1 + \hat{q}_0 = \frac{1}{q_1 - q_0} \quad (30)$$

$$\hat{R} = \frac{R}{q^*(q_1 - q_0)} \quad (31)$$

$$\hat{q}_1 = \frac{q_1 - 2q_0 + R^2/q^*}{(q_1 - q_0)^2} \quad (32)$$

which gives

$$-\beta f = \text{extr}_{q_1, q_0, \hat{q}_0, R} \left[\frac{1}{2} \frac{q_1 - R^2/q^*}{q_1 - q_0} + \frac{1}{2} \ln(q_1 - q_0) + \frac{1}{2} \ln(2\pi) + \alpha \int Dt \ln \left[\int \frac{dk}{\sqrt{2\pi(q_1 - q_0)}} \exp\left\{-\frac{(k - R - \sqrt{q_0}t)^2}{2(q_1 - q_0)} - \beta \rho(k)\right\} \right] \right] \quad (33)$$

We are particularly interested in the low-temperature limit $\beta \rightarrow \infty$; according to (7), this limits project out the couplings minimizing the objective function. In the low-temperature limit we find that the order parameters at the extremum (33) scale as $q_1 - q_0 \rightarrow v/\beta$, where v and q_0 are of order one. With this scaling, the integral over k in (33) can be evaluated by saddle-point integration. To leading order in β we have

$$\ln \left[\int \frac{dk}{\sqrt{2\pi(q_1 - q_0)}} \exp\left\{-\frac{(k - R - \sqrt{q_0}t)^2}{2(q_1 - q_0)} - \beta \rho(k)\right\} \right] = -\beta \min_k \left[\frac{(k - R - \sqrt{q_0}t)^2}{2v} + \rho(k) \right]. \quad (34)$$

The minimum over k admits a simple interpretation: As a function of $x = R + \sqrt{q_0}t$, this is a minimum of $\rho(k)$ that is ‘close’ to x , where the trade-off between closeness and smallness is controlled by v . This relationship plays a central role in convex optimisation [14], where it is known as the Moreau envelope \mathcal{M}_v of a function f

$$\mathcal{M}_v[f](x) = \min_y \left[\frac{(y-x)^2}{2v} + f(y) \right]. \quad (35)$$

With this we obtain

$$-f = \text{extr}_{q,v,R} \left[\frac{q - R^2/q^*}{2v} - \alpha \int Dt \mathcal{M}_v[\rho](R + \sqrt{q}t) \right]. \quad (36)$$

Setting the derivatives of this expression with respect to q, v and R to zero gives the three saddle-point equations

$$\begin{aligned} \frac{1}{v} - \frac{\alpha}{\sqrt{q}} \int Dt t \frac{d\rho}{dk} \Big|_{k=k(R+\sqrt{t})} &= 0 \\ -\frac{R}{q^*v} - \alpha \int Dt \frac{d\rho}{dk} \Big|_{k=k(R+\sqrt{t})} &= 0 \\ -\frac{q - R^2/q^*}{v^2} + \alpha \int Dt \left(\frac{d\rho}{dk} \Big|_{k=k(R+\sqrt{t})} \right)^2 &= 0, \end{aligned} \quad (37)$$

where $k(R+\sqrt{t})$ is value of k attaining the minimum in (34). To derive these equations we used $\partial_x \mathcal{M}_v[\rho](x) = \frac{d\rho}{dk} \Big|_{k=k(x)}$ and $\partial_v \mathcal{M}_v[\rho](x) = -\frac{1}{2} \left(\frac{d\rho}{dk} \Big|_{k=k(x)} \right)^2$.

2. Finding the optimal objective function

We are interested in the particular objective function that when used to reconstruct couplings according to (7), yields reconstructed couplings that are closest to the underlying couplings. We use the relative mean-square error (13) to quantify the performance of a particular objective function. We thus seek the particular function $\rho(k)$ which maximizes $\frac{q-2R+q^*}{\sqrt{qq^*}}$, subject to the constraints (37) specified by the saddle point equations. A similar calculation appears in the context of optimal regression [18]. We use Lagrange multipliers and maximize

$$L = \frac{q - 2R + q^*}{\sqrt{qq^*}} + \gamma_1 \left[\frac{\sqrt{q}}{v} - \alpha \int Dt t \rho' \right] + \gamma_2 \left[\frac{R}{q^*v} + \alpha \int Dt \rho' \right] + \gamma_3 \left[\frac{q - R^2/q^*}{v^2} - \alpha \int Dt (\rho')^2 \right], \quad (38)$$

where we use the shorthand $\rho' = \frac{d\rho}{dk} \Big|_{k=k(x)}$. With $\rho' = \partial_x \mathcal{M}_v[\rho](x)$ we have $\int Dt \rho' = \int D_{R,q} x \mathcal{M}'_v(x)$, $\int Dt t \rho' = \sqrt{q} \int D_{R,q} x \mathcal{M}''_v(x)$ and $\int Dt (\rho')^2 = \int D_{R,q} x (\mathcal{M}'_v(x))^2$ we can write (38) as

$$L = \frac{q - 2R + q^*}{\sqrt{qq^*}} + \gamma_1 \frac{\sqrt{q}}{v} + \gamma_2 \frac{R}{q^*v} + \gamma_3 \frac{q - R^2/q^*}{v^2} + \alpha \int_{-\infty}^{\infty} D_{R,q} x \mathcal{L}(x) \quad (39)$$

with

$$\mathcal{L}(x) = -\gamma_1 \sqrt{q} \frac{d^2 \mathcal{M}_v}{dx^2} + \gamma_2 \frac{d\mathcal{M}_v}{dx} - \gamma_3 \left(\frac{d\mathcal{M}_v}{dx} \right)^2 \quad (40)$$

and $D_{R,q} x$ a shorthand for a Gaussian integral measure with mean R and variance q . To find the optimal $\rho(k)$ we take the functional derivative of L with respect to $\frac{d\mathcal{M}_v}{dx}$, solve the resulting Euler-Lagrange equation, and determine the corresponding $\rho(k)$ by inverting the Moreau envelope (35). The Euler-Lagrange equation

$$\frac{\partial}{\partial \mathcal{M}'_v} (G_{R,q}(x) \mathcal{L}(x)) - \frac{d}{dx} \frac{\partial}{\partial \mathcal{M}''_v} (G_{R,q}(x) \mathcal{L}(x)) = 0 \quad (41)$$

gives

$$\frac{d\mathcal{M}_v}{dx} = \frac{1}{2\gamma_3} \left(\gamma_2 + \gamma_1 \sqrt{q} \frac{d}{dx} \ln G_{R,q}(x) \right), \quad (42)$$

where $G_{R,q}(x)$ is a Gaussian with mean R and variance q . Inserting this result into (40), gives

$$\mathcal{L}(x) = -\frac{\gamma_1^2 q G''_{R,q}}{2\gamma_3} + \frac{\gamma_1^2 q G'^2_{R,q}}{3\gamma_3 G^2_{R,q}} + \frac{\gamma_2^2}{4\gamma_3} . \quad (43)$$

The first term integrates to zero, the second involves $\int_{-\infty}^{\infty} x \frac{G'^2_{R,q}(x)}{G^2_{R,q}(x)} = \frac{1}{q}$ which gives the Lagrangian (39) as

$$L = \frac{q - 2R + q^*}{\sqrt{qq^*}} + \gamma_1 \frac{\sqrt{q}}{v} + \gamma_2 \frac{R}{q^* v} + \gamma_3 \frac{q - R^2/q^*}{v^2} + \alpha \frac{\gamma_1^2 + \gamma_2^2}{4\gamma_3} . \quad (44)$$

Extremization with respect to the Lagrange parameters gives

$$\frac{\sqrt{q}}{v} + \frac{\alpha}{2} \frac{\gamma_1}{\gamma_3} = 0 \quad (45)$$

$$\frac{R}{vq^*} + \frac{\alpha}{2} \frac{\gamma_2}{\gamma_3} = 0 \quad (46)$$

$$\frac{q - R^2/q^*}{v^2} - \frac{\alpha}{4} \frac{\gamma_1^2 + \gamma_2^2}{\gamma_3^2} = 0 . \quad (47)$$

Only the first two of these equations are required to evaluate (42), the third establishes a relationship between the overlaps R and q at the optimal objective function

$$q(1 - 1/\alpha) - \frac{R^2}{q^*} \left(1 - \frac{1}{\alpha q^*}\right) = 0 . \quad (48)$$

Integrating (42) now gives up to a constant

$$\mathcal{M}_v[\rho](x) = -\frac{1}{\alpha v} \left(\frac{R}{q^*} x - \frac{1}{2} (x - R)^2 \right) , \quad (49)$$

from which the optimal objective function can be obtained easily based on the relation that for a convex function $f(y)$, $\mathcal{M}[f]_v(x) = g(x)$ implies $f(y) = -\mathcal{M}[-g]_v(y)$. Inverting (49) gives again up to a constant

$$\rho_{\text{opt}}(k) = \frac{1}{\alpha} \left(k - \frac{R(1 + q^*)}{q^*} \right)^2 . \quad (50)$$

The optimal value of R is specified by extremizing the Lagrangian (38), giving $q = q^*$.

Of course q^* is not known when reconstructing the couplings. We set out with a free parameter δ as the offset, which needs to be determined, so

$$\rho_{\text{opt}}(k) = k^2 - 2\delta k . \quad (51)$$

The free energy for this particular objective function is

$$-f = \text{extr}_{q,v,R} \left[\frac{q - R^2/q^*}{2v} - \alpha \frac{R^2 + q - 2R\delta - 2\delta^2 v}{2v + 1} \right] . \quad (52)$$

with saddle-point equations giving

$$v = \frac{1}{2(\alpha - 1)} \quad (53)$$

$$R = \frac{q^* \delta}{1 + q^*} \quad (54)$$

$$q = \frac{\alpha q^* + 1}{(1 + q^*)^2 (\alpha - 1)} \delta^2 . \quad (55)$$

The last result is crucial as the overlap q of reconstructed couplings can be computed without knowing the underlying couplings. q^* can be determined from a simple linear fit of q against δ^2 , which determines the offset parameter in the optimal objective function

$$\delta = (1 + q^*) \sqrt{\frac{q^*(1 - \alpha)}{\alpha q^* + 1}} . \quad (56)$$

3. The distribution of couplings

The statistics of reconstructed couplings can be read off from the free energy (26) using standard arguments, giving the average fraction of couplings exceeding a threshold a as

$$\int D_{q^*} J^* \int Dt \frac{\int_a^\infty dJ \exp\{-\frac{1}{2}(\hat{q}_0 + \hat{q}_1)J^2 + \sqrt{\hat{q}_0}tJ + \hat{R}J^*J\}}{\int_{-\infty}^\infty dJ \exp\{-\frac{1}{2}(\hat{q}_0 + \hat{q}_1)J^2 + \sqrt{\hat{q}_0}tJ + \hat{R}J^*J\}}. \quad (57)$$

For the low-temperature limit we use the scaling of the conjugate order parameters (30)

$$\begin{aligned} \hat{q}_1 + \hat{q}_0 &= \beta/v \\ \hat{q}_0 &= \frac{\beta^2}{v^2}(q_0 - R^2/q^*) \\ \hat{R} &= \frac{\beta R}{vq^*}, \end{aligned} \quad (58)$$

which turns the integrals over J into saddle-point integrals with saddle-point equation

$$J = \frac{RJ^*}{q^*} + \sqrt{q - R^2/q^*}t. \quad (59)$$

Since t follows a Gaussian with mean zero and unit variance, this result means that the reconstructed coupling J is on average $\frac{RJ^*}{q^*}$ (specifying the bias) and variance $q - R^2/q^*$.

Similarly, the distribution of k^μ can be calculated, in the low-temperature limit their statistics is that of

$$\operatorname{argmin}_k \left[\frac{(k - R - \sqrt{q_0}t)^2}{2v} + \rho(k) \right] \equiv \mathcal{P}_v[\rho](R + \sqrt{q}t), \quad (60)$$

where t is a univariate Gaussian with zero mean. $\mathcal{P}_v[\rho](x)$ is called the proximal map [14].